Surface Characterization of Titanium-Based Implant Materials

Hallie E. Placko, MSE[1]/Sourabh Mishra, PhD[2]/Jeffery J. Weimer, PhD[3]/Linda C. Lucas, PhD[4]

This study examined the effects of different treatments (polished, electropolished, and grit-blasted) on the surface morphology and chemistry of commercially pure titanium and titanium-6% aluminum-4% vanadium. The structure and composition of the surfaces were evaluated using scanning electron microscopy, atomic force microscopy, energy dispersive spectroscopy, Auger microprobe analysis, and x-ray photoelectron spectroscopy. Surface roughness values at large scales were nearly identical for grit-blasted and electropolished samples, while at smaller scales, electropolished and polished samples had nearly identical quantitative roughness values. The surface oxide compositions were found to be primarily titanium dioxide on both materials for all surface treatments. No vanadium was seen with either x-ray photoelectron spectroscopy or Auger microprobe analysis for the alloy, indicating a possible surface depletion. Calcium was present on the grit-blasted samples, and calcium and chlorine were detected on the electropolished samples. (INT J ORAL MAXILLOFAC IMPLANTS 2000;15:355–363)

Key words: *characterization, dental implants, surface properties, titanium*

The study of biomedical implant surfaces and the effects of surface modifications has become popular in recent years because of the consideration that surface characteristics directly influence biomaterial-tissue interactions. The contribution of biomaterial surface properties to in vivo function can be illustrated by commercially pure titanium (cpTi), which has excellent biocompatibility and biologic acceptance in bone. Studies have shown the direct apposition of bone to cpTi surfaces, which results in cellular attachment and implant stability.[1] These characteristics have been attributed to the presence of an oxide layer that forms spontaneously on the surface of cpTi. The stability of this passive oxide layer is also responsible for the high corrosion resistance of cpTi.

Many studies have been directed toward defining the nature of the interactions between the oxide layer on cpTi and the surrounding tissue and toward investigating the biologic effects of treatments in which the surface can be modified to hold specific properties. Although the potential may exist to prepare a controlled surface with specified properties, the desired characteristics are not completely defined or understood. The combination of the effects of surface morphology and surface chemistry must be considered. Other important factors include thickness and structure of the passive layer and the levels of contaminant present on the surface. In addition, alloying titanium with other materials can change the characteristics of the surface and oxide, which may result in altered tissue response.

The effects of surface roughness of the formation of the oxide layer and cellular adhesion have been studied.[2,3] Although the nature of the oxide surface of cpTi and titanium-6% aluminum-4% vanadium (Ti-6Al-4V) appears to be similar, some differences are observed that may have biologic implications. Using several surface analysis techniques, Keller et al[2] found the oxide on Ti-6Al-4V alloys to be significantly thicker than that on cpTi samples. This difference was not determined to be biologically significant. Cell attachment seemed to favor roughened sandblasted surfaces (Ra = 0.7 μm to 0.9 μm) as compared to polished (Ra = 0.04 μm) or grooved specimens (Ra = 0.1 μm to 0.2 μm). No difference

[1]Graduate Fellow, Department of Biomedical Engineering, University of Alabama at Birmingham.
[2]Researcher, Joint Materials Science PhD Program, University of Alabama at Huntsville.
[3]Adjunct Associate Professor, Joint Materials Science PhD Program, University of Alabama at Huntsville.
[4]Professor and Chair, Department of Biomedical Engineering, University of Alabama at Birmingham.

Reprint requests: Hallie E. Placko, Department of Biomedical Engineering, University of Alabama at Birmingham, 1075 13th St. S., Hoehn 370, Birmingham, Alabama 35294. Fax: (205) 975-4919. E-mail: placko@atax.eng.uab.edu

was seen between cpTi and Ti-6Al-4V materials with respect to cellular attachment.

Several studies have examined the effects of specific surface treatments on the composition and structure of the oxide layer for titanium-based materials. According to Lausmaa et al,[4,5] oxides on cpTi and Ti-6Al-4V that have been formed by machining or electropolishing consist mainly of titanium dioxide (TiO_2) with oxygen, carbon, and nitrogen species present as contaminants. Inorganic contaminants included small amounts of sodium, chlorine, silicon, calcium, phosphorous, and sulfur; however, these elements were not detected on all specimens. Aluminum was also observed in the oxide on the alloy, and vanadium was not found on any specimens. Samples with oxide thicknesses less than 100 nm were found to be amorphous. Above this value, a structured rutile oxide was formed. Mausli et al[6] found that halides and other impurities can be trapped in the oxide layer during some oxidative heat treatments. A study of the dissolution resistance of Ti-6Al-4V revealed a decrease in metal ion release with thermal treatment resultant to the formation of a more stable rutile oxide structure.[7] This phenomenon was enhanced on rough surfaces because of the increased surface area.

Although many studies have incorporated the effects of surface treatments on the composition and structure of the oxide, few have examined the differences between the combined effects of treatment and alloying. The objective of this study was to examine the oxide layers for 3 surface treatments—mechanically polished, electropolished, and grit-blasted—on the 2 materials, cpTi and Ti-6Al-4V. Several methods of surface characterization were employed. Surface morphology was examined by scanning electron microscopy (SEM) and atomic force microscopy (AFM), and chemical composition was determined using energy dispersive spectroscopy (EDS), Auger microprobe analysis (AES), and x-ray photoelectron spectroscopy (XPS).

MATERIALS AND METHODS

Samples were made from grade 4 cpTi and Ti-6Al-4V rod stock approximately 6 mm in diameter. Sections were cut from the rod into disks 1 to 3 mm wide, embedded in black phenolic compression molding powder, and ground to 600 grit on silicon carbide paper. Ground samples were then polished to a 1-μm finish. Electropolishing was conducted as described by Lausmaa et al,[5] and grit-blasted samples were removed from the mold and blasted with a calcium phosphate material (Biocoat Inc, Southfield, MI). Following removal from the mold, all samples were sonically cleaned in 95% ethanol for 10 minutes and rinsed in distilled water prior to passivation in 20% nitric acid for 30 minutes as per ASTM F86. Samples were stored in individual vials and sonically cleaned in ethanol for several minutes just before analysis.

Surface Morphology

One set of treatments (grit-blasting, electropolishing, and polishing) of each type of sample (cpTi and Ti-6Al-4V) was examined by SEM on a Phillips 515 scanning electron microscope (Phillips Analytical, Natick, MA) with an accelerating voltage of 30 kV to determine surface morphology for each material and surface preparation. Representative photomicrographs were taken from each sample group.

One representative sample from each group was scanned with AFM (Nanoscope III, Digital Instruments, Santa Barbara, CA) in tapping mode using standard silicon tips with a nominal tip radius of 20 nm. Two regions were imaged on each sample. For each region, scans were done in a sequence of sizes ranging from 200 mm × 200 mm to 0.1 μm × 0.1 μm. The scan rate was about 0.1 Hz at the largest size and about 10 Hz or less for the smallest scan (faster scans were possible on smoother surfaces). All images were taken with a resolution of 512 × 512 pixels. The data resolution normal to the image plane was adjusted to be the best possible under the given scan conditions, accounting for sample tilt and the height of surface features. The raw images were all fit into a quadratic plane in the x and y directions to remove image distortion. Where appropriate, the image was also flattened with a zero-order line fit to remove scan line anomalies. Roughness values were calculated for each corrected image over the entire image frame. For display purposes, the images were also passed through a low-pass filter to remove spurious noise.

Chemical Analysis

The set of samples examined by SEM were also analyzed by EDS (KEVEX 8000) to verify bulk compositions of the materials. Chemical analyses were conducted on 2 areas per sample.

Three samples of each type were examined by AES (JEOL JAMP-30, Tokyo, Japan) with an electron beam voltage of 10 kV and a beam current less than 3×10^{-7} A. Differential spectra were collected at 2 areas for each sample. Atomic concentrations were determined using the relative sensitivity factors for 10 kV. Concentration ratios were calculated using peak height intensities corrected by the appropriate relative sensitivity factors. A depth profile was also collected for 1 of the 3 samples using a sputter interval of 2 seconds. The sputtering rate, obtained

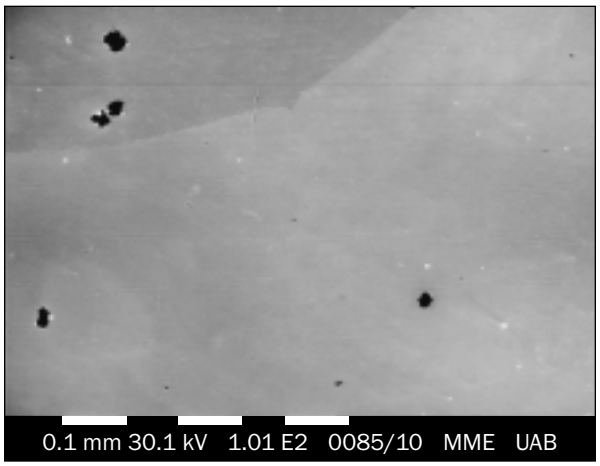

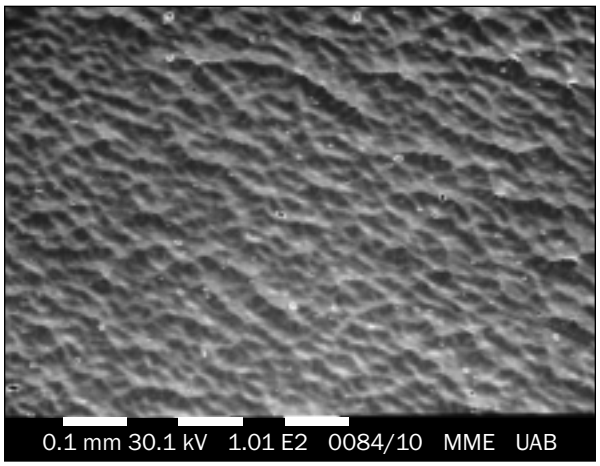

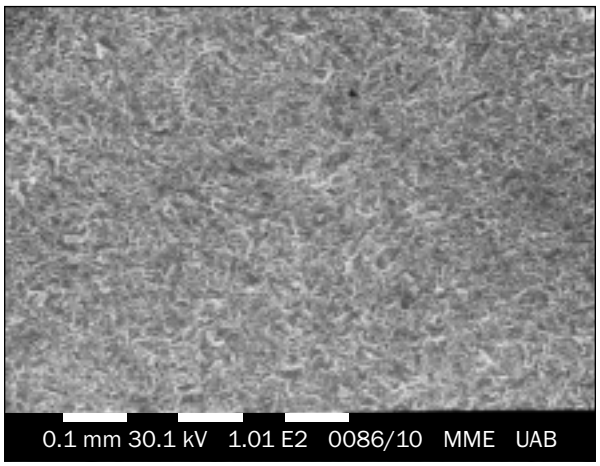

Figs 1a to 1c Photomicrographs (SEM) of treated surfaces (original magnification ×100). (*Above*) Polished cpTi; few scratches are evident with some voids present. (*Above right*) Electropolished cpTi; note wavy morphology of the surface. (*Right*) Grit-blasted cpTi; note visibly roughened surface with pits and flakes.

from sputtering of a 100-nm film of Ta_2O_5 under the same sputtering conditions, was 0.32 nm/s.[8,9]

X-ray photoelectron spectroscopy measurements were performed using a Physical Instruments 5400 spectrometer (Perkin-Elmer, Wellesley, MA). All scans were conducted with a Mg Kα x-ray source with an angle of acquisition of 45 degrees to the sample. Survey scans were taken from 3 specimens from each group at a pass energy of 89.45 eV and a scan resolution of 0.5 eV/step. High-resolution scans were taken for 2 samples per treatment at a pass energy of 8.95 eV and scan resolution of 0.05 eV/step. High-resolution spectra were shifted so that the main C 1s peak fell at 286 eV to account for differential charging of the samples. Smooth curves shown in the high-resolution spectra were generated by fast Fourier transform filtering of the noise from the spectra. Peak fitting was done for the O 1s high-resolution data. Prior knowledge of the surface chemistry was used to select a minimum set of appropriate component peaks for the fitting process. The objective was to get an estimate of the surface chemistry. Before peak fitting, an integrated baseline[10] was subtracted in all cases. Peak fitting was done using Gaussian peaks with a variable fraction of the Lorentzian component. The position, height, and full width at half maximum (FWHM) were standard fitting parameters. No attempts were made in this work to go beyond fitting of the minimum set of peaks.

RESULTS

Surface Morphology

The SEM images revealed differences in surface morphology, as seen in the representative images in Figs 1a to 1c. No differences were seen between cpTi and Ti-6Al-4V for each surface treatment. However, significant differences were observed between different treatments for the same material. The polished surfaces (Fig 1a) were relatively free of scratches, while the electropolished surfaces (Fig 1b) appeared to have a wavy morphology, with some porosity and spherical pits. The grit-blasted surface was visibly roughened, with many cracks and pits in the metal (Fig 1c).

Figs 2a to 2f Atomic force microscopy images with a scan size of 1 μm × 1 μm.

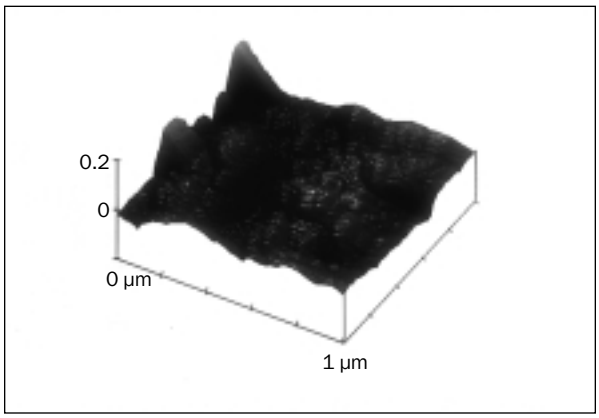

Fig 2a Grit-blasted cpTi.

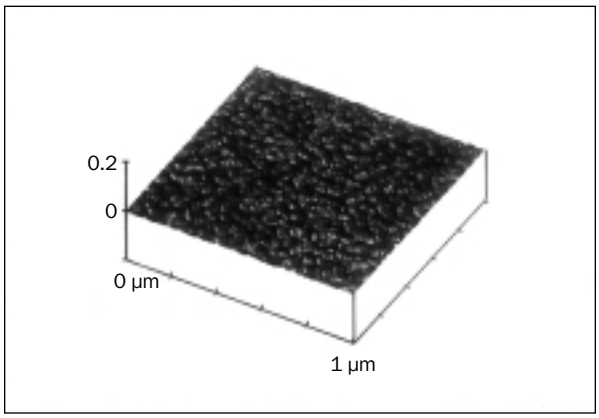

Fig 2b Electropolished cpTi.

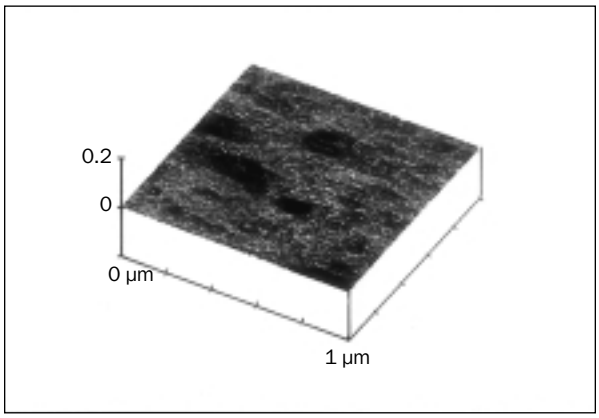

Fig 2c Polished cpTi.

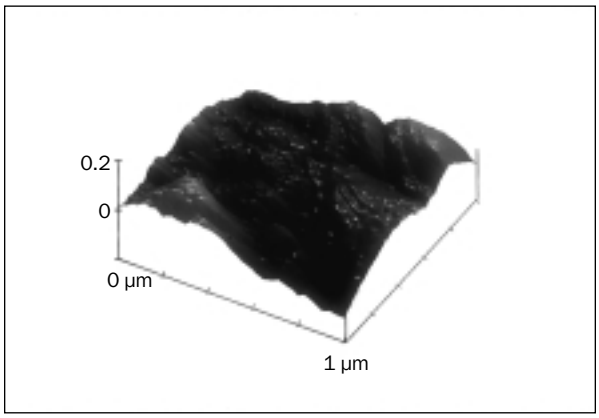

Fig 2d Grit-blasted Ti-6Al-4V.

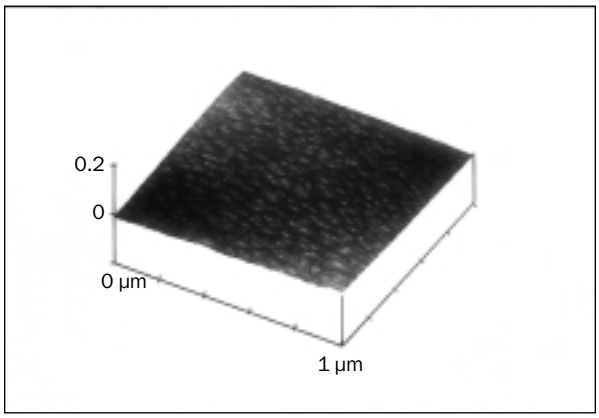

Fig 2e Electropolished Ti-6Al-4V.

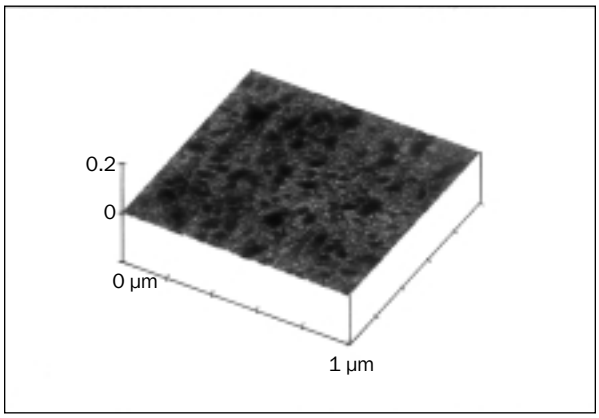

Fig 2f Polished Ti-6Al-4V.

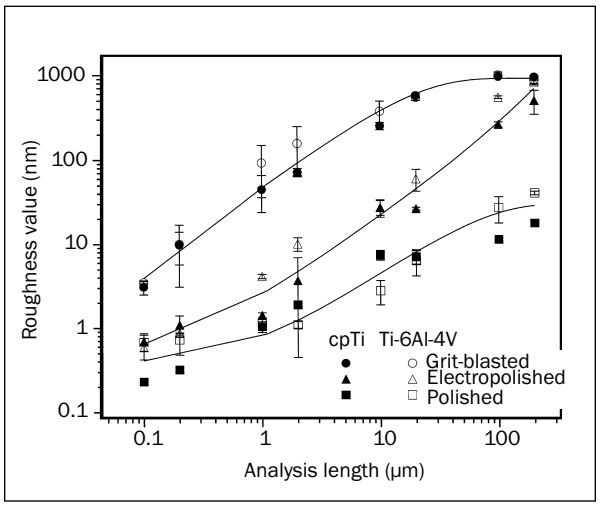

Fig 3 Root mean square roughness values for atomic force microscopy scans.

Table 1 Bulk Composition (%) of Ti-6Al-4V Alloy Samples as Determined by Energy Dispersive Spectroscopy

Treatment	Ti	Al	V
Grit-blasting	92	5	3
Electropolishing	92	5	3
Polishing	92	6	3

Values are the average of 2 measurements and have relative errors of about 10%.

Figures 2a to 2f show the AFM images with a scan size of 1 μm × 1 μm. As with the SEM results, the surfaces appear nearly the same for cpTi and Ti-6Al-4V materials for a given surface treatment. Further details of the topography were seen at higher magnifications. The grit-blasted samples had sharply defined features, the polished samples showed striations and pits, and the wavy texture of the electropolished samples, as seen with SEM, was found to be the result of etched grains.

Root mean square (RMS) roughness values determined from scans with AFM are shown in Fig 3. The values are plotted versus the length of one side of the (square) image frame. This length is proportional to the pixel resolution in the plane of the image according to the formula: image resolution = scan length/512. The data points are average values for the 2 regions scanned, and the error bars represent the differences between the maximum and minimum values measured. Error bars that are not shown are smaller than the size of the point. The solid curves show the overall trends in the data for the 3 sets of samples (GB, EP, and PL) when both Ti types (commercially pure and alloy) were considered together. The mean roughness values were lower in all cases than the RMS values shown in Fig 3, and qualitatively they followed the same trends. For clarity, the mean roughness values are not shown. The roughness values were generally lowered by the off-line flattening process, in some cases by as much as 30%. In most cases, the 2 values measured for each region differed by more than the change caused by flattening, and the error bars and scatter in data points in Fig 3 encompassed the variations.

Chemical Analysis

The EDS results were similar for both materials, with titanium being the only detectable element in all of the cpTi samples. The compositions for the alloy are given in Table 1. The results revealed small amounts of aluminum and vanadium, as expected. The weight percents do not correlate precisely with the stoichiometry of the alloy (6% Al and 4% V) but are within the range of uncertainty when considering the roughness of the sample preparations and inherent error of the system. Bulk composition did not vary with surface treatment.

Analysis with AES revealed oxygen, titanium, and carbon on the surfaces of both cpTi and Ti-Al-4V. The atomic concentrations are shown in Table 2. A representative spectrum from an electropolished cpTi sample is shown in Fig 4, with the O, C, Ti, Ca, and Cl peaks labeled. For all samples, oxygen was the highest concentration on the surface. Carbon appeared to be lowest on electropolished samples. For all polished and grit-blasted surfaces, the concentrations of O, C, and Ti were similar. Additional contaminants included trace amounts of Ca found on the surface of all grit-blasted samples and similar amounts of Ca and Cl on the electropolished samples. Although the electropolished surfaces appeared to have the highest O and lowest C concentrations, further analysis is warranted to improve the statistics. The O/Ti ratio determined by AES was in the range of 5.5 to 7, while the C/Ti ratio was in the range of 1 to 2, as shown in Table 2.

The XPS survey scans were used to determine atomic concentrations. The values are shown in Table 3. They show significantly higher carbon

Table 2 Atomic Concentrations and Ratios as Determined by Auger Microprobe Analysis

	Atomic concentrations (%)					Concentration ratios	
Sample	O	C	Ti	Al	Trace (< 1%)	O/Ti	C/Ti
cpTi							
Grit-blasted	68	19	11	—-	Ca	6.4	1.8
Electropolished	73	16	13	—	Ca, Cl	5.5	0.9
Polished	69	19	12	—-	—	5.7	1.6
Ti-6Al-4V							
Grit-blasted	69	18	10	3	Ca	7.0	1.6
Electropolished	74	10	12	2	Ca, Cl	6.1	0.8
Polished	66	20	10	3	—	6.4	2.0

Values are averages from 3 samples, with a relative error of approximately 10% for atomic concentrations and 20% for concentration ratios.

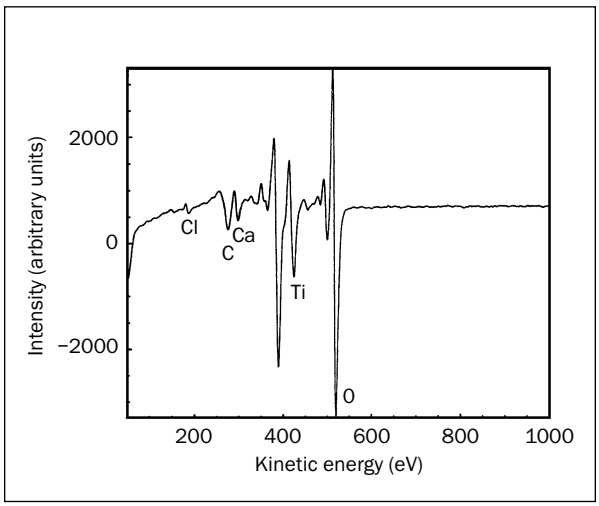

Fig 4 Typical Auger microprobe analysis spectrum of electropolished cpTi sample. Note characteristic peaks for Ti, O, C, Ca, and Cl.

concentrations on the surfaces than was determined by AES. Since XPS probes deeper into the surface of a material, this means that carbon concentrations increase as one progresses further into the material. The oxygen concentration is also lower in XPS than in AES, suggesting that the immediate surface layer of the samples is more highly oxidized than deeper into the bulk. The O/Ti and C/Ti ratios in Table 3 were determined from the concentrations in the survey scans.

Representative high-resolution Ti 2p, O 1s, and C 1s spectra for each surface and material are shown in Figs 5a to 5c. The Ti 2p peak consists of a large contribution at 459 eV, corresponding to TiO_2.[4,5,10–12] Metallic Ti appears at about 465 eV, and Ti suboxides (TiO or Ti_2O_3) appear as a shoulder to the main TiO_2 peak at about 457 eV.[10–14] The O 1s peak (Fig 5b) shows a characteristic peak for TiO_2 at 531 eV. The shoulder in the range of 532 eV to 534 eV can be attributed to impurities such as H_2O, as well as CO and OH groups on the surface.[10,13,15] The spectra from the grit-blasted samples had a significant shoulder, indicating a larger amount of oxygen-containing contaminants as compared to the other surface treatments. The C 1s peaks (Fig 5c) show the nature of the carbonaceous contaminants. In this case, a single hydrocarbon peak at 286 eV dominates for all samples, indicative of primarily carbonaceous-type impurities.

Relative concentration ratios of oxygen-containing species were determined by curve-fitting the O 1s spectra in Fig 5c to 2 peaks with 90% Gaussian character. A peak at 531.6 ± 0.6 eV represented the TiO_2 species. The FWHM of this peak was held constant at 1.5 eV during the fitting. A peak at 533.5 ± 0.7 eV represented other oxygen-containing species. The FWHM of this peak varied between 1.9 eV and 2.4 eV because it represents a wider range of oxygen-containing species, such as hydroxide and carbonyl groups. The fitting procedure did not always give an optimal fit to the raw data; in some cases, other components were clearly needed to minimize the residual. These components would include suboxides of titanium as well as oxygen-containing species that are not well represented by the single envelope at 533.5 eV. No attempt was made to add further O 1s component peaks during the fitting for this work.

The relative area of the peak for TiO_2 (531 eV) was used to determine the $O(TiO_2)/Ti$ ratios given in Table 3. All ratios of $O(TiO_2)/Ti$ were more than 2, with the values closest to 2 occurring for the electropolished samples for both materials. The total O/Ti and C/Ti ratios were highest on the grit-blasted samples, regardless of the material. For cpTi, the O/Ti and C/Ti ratios were lowest for the polished specimens, while for Ti-6Al-4V, the same was true for the electropolished samples.

Table 3 Atomic Concentrations and Concentration Ratios as Determined by X-ray Photoelectron Spectrophotometry

	Atomic concentrations (%)			Concentration ratios		
Sample	**O**	**C**	**Ti**	**O/Ti**	**C/Ti**	**O(TiO_2)/Ti**
cpTi						
Grit-blasted	44	47	9	4.9	5.2	2.2
Electropolished	41	47	12	3.4	3.9	1.5
Polished	50	40	11	4.4	3.7	3.0
Ti-6Al-4V						
Grit-blasted	35	55	7	4.8	5.3	3.0
Electropolished	45	40	14	3.3	2.9	2.3
Polished	43	48	9	4.8	5.3	3.0

Values are averages from 3 samples, with a relative error of approximately 10% for atomic concentrations and 20% for concentration ratios.

Figs 5a to 5c X-ray photoelectron spectroscopy peaks representative of all sample types. GB = grit-blasted; EP = electropolished; PL = polished.

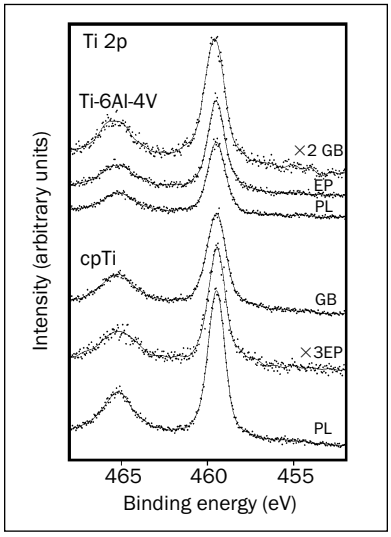

Fig 5a Typical Ti 2p peaks; note the metallic Ti peak at approximately 465 eV and the characteristic oxide peak at 459 eV.

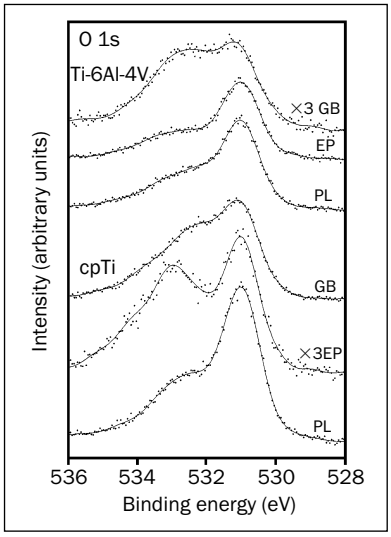

Fig 5b Typical O 1s peak; note oxide peak (TiO_2) at 531 eV and the shoulder at 532 eV because of impurities such as H_2O and CO and OH groups.

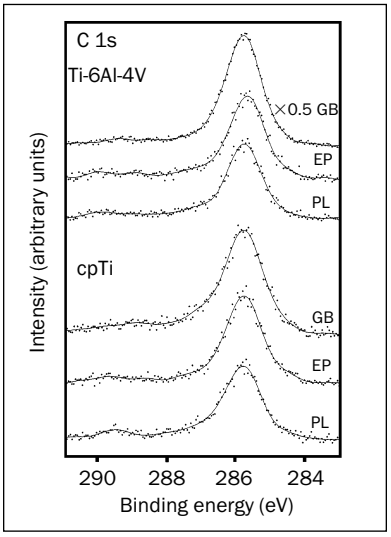

Fig 5c Typical C 1s peak; note main peak at ≈286 eV resulting from carbonaceous impurities and adsorbed hydrocarbons.

DISCUSSION

The SEM and AFM analyses show that few if any differences exist between the cpTi and Ti-6Al-4V samples for any given surface treatment. Significant differences are seen in surface topography among the 3 treatments. As seen by the sequence of images from SEM in Figs 1a to 1c and AFM in Figs 2a to 2f, the grit-blasted samples tend to have sharply defined step edges, ledges, and peaks at all length scales; the electropolished samples have etch pits on the order of a few μm in diameter and are otherwise covered with a texture indicative of selective etching at grain boundaries; and the polished samples contain striations and pits that appear to have arisen from the mechanical polishing process.

Differences in surface topography resulting from treatment are also apparent when roughness values are compared quantitatively as in Fig 3. At large length scales (greater than 100 μm), polishing produces the smoothest surfaces, with RMS roughness values about 2 orders of magnitude smaller than the other 2 surface treatments. On smaller length scales (1 μm and below), both the polished

and electropolished samples have comparable if not the same RMS roughness values, while the grit-blasted samples are as much as an order of magnitude rougher.

The results shown in Figs 1 to 3 are of significant importance in further considerations of the role of mechanical binding versus chemical bonding as factors in promoting strong adhesion of coatings, bone, or tissue to an implant surface. On the qualitative side, the role of sharp step edges, etch pits, textured grains, and striations should be different in both mechanical bonding and cell growth or adhesion phenomena. When considered from the quantitative side, tests to determine whether coating adherence or cell growth is affected by surface roughness will have to consider the length scale that is critical during these processes. For example, bone cells have been shown to grow aligned with surface ridges that are as small as 2 μm and as large as 10 μm in size.[16] The results shown in Fig 3 confirm that this is a critical range in which the 3 treatments produce surfaces of quantitatively different roughness values. In addition, although surfaces may have the same quantitative roughness values, they can have dramatically different surface textures, as seen by comparison of the electropolished and polished samples for length scales of 1 μm. This further complicates any quantitative analysis of how roughness affects cell growth or coating adhesion. Finally, the results shown in Figs 1 to 3 are expected to vary both qualitatively and quantitatively according to other parameters involved in the surface treatment process. For mechanical polishing, the time spent at each grit size, the type of grit used (eg, diamond versus alumina), the pressure applied during polishing, and the final grit size will all play a role in determining the smoothness of the surface. For electropolishing, the time in solution, the degree of polishing beforehand, the type of solution, and the etch rate will be important.

From the XPS spectra, the $O(TiO_2)/Ti$ ratio was close to or greater than 2 for all samples. The majority of the oxide on the surface can therefore be assumed to be TiO_2 for all surfaces. Slightly higher values (closer to 3) have been reported by other investigators for similar surfaces.[2] In addition, the Ti peak shape on all samples is qualitatively similar to those reported for TiO_2 samples,[5] and the Ti 2p peak at about 459 eV on all samples agrees with reported values for TiO_2.[10–14] The Ti Auger peak (doublet) found on all samples (see Fig 4) was similar in shape to the spectra reported by Lausmaa et al,[4,5] which is considered to be characteristic of TiO_2.

Trace elements were detected on the grit-blasted or electropolished surfaces only by AES. These findings can be attributed to the fact that Auger electrons are collected from only the first few atomic layers, whereas the signals for XPS are collected from deeper atomic layers. This results in different sensitivity for specific elements on the topmost surfaces of the material. The calcium contamination found on all grit-blasted samples probably arose from the grit-blasting process. This process involved bombarding the surface with a calcium phosphate material, with a cleaning step to dissolve away any embedded material. Calcium was also detected on the surface of the electropolished samples, along with chlorine. The electropolishing solution contained approximately 6% perchloric acid. Chlorine may have been trapped on the surface during the electropolishing treatment. Lausmaa et al[5] also found calcium contamination throughout the thickness of the oxide layer of electropolished specimens; however, they did not speculate as to the origin of this contamination. It is interesting to note that Lausmaa and coworkers found these elemental contaminants as well as others using XPS, whereas in this study, these contaminants were detected only with AES capabilities.

Aluminum was detected by AES for all of the alloy specimens but was not detected by XPS. This discrepancy may also have been the result of the greater surface sensitivity of AES, suggesting that aluminum is surface-segregated on the Ti-6Al-4V alloy. The vanadium concentration detected with AES was lower than expected, and no vanadium was seen with XPS. This may indicate depletion of vanadium from the alloy surface. The AES spectra also showed the electropolished surfaces as being somewhat "cleaner" than either the polished or grit-blasted surfaces, with less carbon and more oxygen present than with the other surface treatments.

The carbon contamination on the surfaces was most likely the result of the adsorption of organic molecules onto the surface during sonic cleaning with ethanol. Peak-fitting of the C 1s envelope showed that 3 components were adequate to represent the spectra in all cases. The primary component at around 286 eV was from aliphatic or graphitic carbon. Components at higher binding energy generally represented about 15% to 20% of the total carbon concentration. A component at around 287 eV to 288 eV was likely from ether or carbonyl carbons, and one at around 289 eV to 290 eV was probably from esters, ketones, or carbonates. The relative amounts of each component were nearly the same on all samples.

Some of the samples for XPS analysis had been exposed to air for prolonged periods of time before analysis. For this reason, the atomic concentrations and concentration ratios do not agree with values from similar Ti studies found in the literature.[2,6] However, the high-resolution data (curve shapes)

obtained for this study are consistent with curves reported elsewhere.[4,5]

The results of the AES depth profiles gave a thickness of the oxides on the specimens of about 3 nm. The alloyed grit-blasted samples appeared to have thicker oxide layers (5 nm). These values fall within a range reported elsewhere for other samples examined in the same AES and XPS system.[12] Oxide thickness values determined by sputter profiling in AES or XPS can be significantly inaccurate if the amplitude of the surface roughness is larger than the true oxide thickness over the scale of the sputtering or analysis beam. Given the results shown in Fig 3, care must be exercised in claiming that any differences exist in the actual oxide thickness from sample to sample.

CONCLUSIONS

The surface morphology and composition of commercially pure titanium and titanium alloys (Ti-6Al-4V) were examined with a range of microscopic and spectroscopic techniques after 3 different surface preparations: grit-blasting, polishing, and electropolishing. The surface morphologies of the samples were nearly the same for a given treatment regardless of the type of material treated. Grit-blasted materials had large protrusions with sharp edges, polished samples were smoother with striations, and electropolished samples had etch pits. Roughness values were dependent on the size of the scan range. At large scales (greater than 100 μm), the grit-blasted and electropolished samples were the same. At small scales (at and below 1 μm), the electropolished and polished samples were the same. Quantitative values of roughness depended significantly on the resolution of the measurement.

Composition at the surface of both materials was dependent more on the type of surface treatment than on the type of material. In general, the surfaces of all the samples consisted mainly of TiO_2, with organic contamination at the surface. Trace amounts of inorganic contamination were found on grit-blasted samples.

ACKNOWLEDGMENTS

The authors would like to acknowledge Wesley Perry for his assistance with the Auger microprobe analysis and scanning electron microscopy. This work was supported by the National Science Foundation—Experimental Program for Stimulation of Competitive Research and Biohorizons Implant Systems, Inc. Student support was provided by the Whitaker Foundation.

REFERENCES

1. Brånemark P-I. Osseointegration and its experimental background. J Prosthet Dent 1983;50:399–410.
2. Keller JC, Stanford CM, Wightman JP, Draughn RA, Zaharias R. Characterization of titanium implant surfaces. III. J Biomed Mater Res 1994;28:939–946.
3. Bowers KT, Keller JC, Randolph BA, Wick DG, Michaels CM. Optimization of surface micromorphology for enhanced osteoblast responses in vitro. Int J Oral Maxillofac Implants 1992;7:302–310.
4. Lausmaa J, Ask M, Rolander U, Kasemo B. Preparation and analysis of Ti and alloyed Ti surfaces used in the evaluation of biological response. Mater Res Soc Symp Proc 1989;110: 647–653.
5. Lausmaa J, Kasemo B, Rolander U, Bjursten LM, Ericson LE, Rosander K, Thomsen P. Preparation, surface spectroscopic and electron microscopic characterization of titanium implant materials. In: Ratner BD (ed). Surface Characterization of Biomaterials. Amsterdam: Elsevier, 1988:161–174.
6. Mausli PA, Simpson JP, Burri G, Steinemann SG. Constitution of oxides on titanium alloys for surgical implants. In: de Putter C, de Lange GL, de Groot K, Lee AFC (eds). Implant Materials in Biofunction: Proceedings of the Seventh European Conference on Biomaterials. Advances in Biomaterials, vol 8. Amsterdam: Elsevier, 1988:305–310.
7. Browne M, Gregson PJ. Surface modification of titanium alloy implants. Biomaterials 1994;15:894–898.
8. Keller JC, Draughn RA, Wightman JP, Dougherty WJ, Meletiou SD. Characterization of sterilized CP titanium implant surfaces. Int J Oral Maxillofac Implants 1990;5:360–367.
9. Swart KM, Keller JC, Wightman JP, Draughn RA, Stanford CM, Michaels CM. Short-term plasma-cleaning treatments enhance in vitro osteoblast attachment to titanium. J Oral Implantol 1992;18:130–137.
10. Briggs D, Seah MP. Practical Surface Analysis: Auger and X-ray Photoelectron Spectroscopy. New York: John Wiley & Sons, 1995.
11. Ong JL, Lucas LC, Lacefield WR, Rigney ED. Structure, solubility and bond strength of thin calcium phosphate coatings produced by ion beam sputter deposition. Biomaterials 1992;13:249–254.
12. Ong JL, Lucas LC, Raikar GN, Gregory JC. Electrochemical corrosion analyses and characterization of surface modified titanium. Appl Surf Sci 1993;72:7–13.
13. Lausmaa J, Kasemo B, Mattsson H. Surface spectroscopic characterization of titanium implant materials. Appl Surf Sci 1990;44:133–146.
14. Lausmaa J, Kasemo B, Mattsson H, Odelius H. Multi-technique surface characterization of oxide films on electropolished and anodically oxidized titanium. Appl Surf Sci 1990; 45:189–200.
15. Pan J, Thierry D, Leygraf C. Electrochemical and XPS studies of titanium for biomaterial applications with respect to the effect of hydrogen peroxide. J Biomed Mater Res 1994;28:113–122.
16. den Brader ET, de Ruijter JE, Smits HTJ, Ginse LA, von Recum AF, Jansen JA. Effect of parallel surface microgrooves and surface energy on cell growth. J Biomed Mater Res 1995;29:511–518.